Ring Buckling of Inflated Drag Bodies

A. D. TOPPING*
Goodyear Aerospace Corporation, Akron, Ohio

Buckling instability may occur in at least three types of aerodynamic decelerators, toroidal drag bodies, drag cones, and the tucked-back balloon-parachute (Ballute).† Buckling criteria for inflated compression members are reviewed, and tests of inflated columns of Mylar, Dacron-neoprene, and stainless steel-silicone fabrics are reported in support of the theoretical development. The theory is then extended to the buckling of a ring in and out of the plane of its centerline. A drag body consisting of a simple torus connected by a skirt to a forebody is used as an illustrative example.

Nomenclature

A = enclosed cross-sectional area
P = axial load
P_c = critical buckling load
P_{ce} = critical buckling load for eccentric column
P_E = Euler buckling load
P_{cr} = local crippling load
L = effective column length
E = modulus of elasticity
E_t = tangent of modulus of elasticity
I = moment of inertia
G = shearing modulus of elasticity
G_o = value of G when $f_t = 0$
G' = shearing modulus of elasticity based on enclosed cross-sectional area
p = gage pressure
f_t = tensile stress
f_{cr} = local crippling stress
r = radius of circular cross-section
R = radius of ring centerline
k,n = section shape factors
$\lambda = pA + kG_o$
N_c = critical radial compressive load per unit length of ring centerline
J = section torsion constant
e = maximum deviation of column centerline from load axis
a = distance from one end to kink
$j = (P/EI)^{1/2}$
t = thickness
c = distance to outermost fiber from neutral axis
s = peripheral length

Introduction

IT may not be apparent that Euler buckling problems exist in aerodynamic decelerators. Actually, they need be considered only in certain types, for example, toroidal drag bodies, drag cones, and tucked-back Ballutes (see Fig. 1). This paper is confined to the first of these types as the one most clearly illustrating the ring buckling problem.

A typical inflatable toroidal drag body consists of an inflated torus connected to a forebody carrying the payload by a skirt having anticlastic curvature. The tension in the skirt where it attaches to the torus has a radial component as well as a component opposed to the drag and normal to the plane of the torus centerline. The radial component produces a hoop compression in the torus that is resisted by a uniform circumferential tension in the skin created by pressure and by the compressive resistance of the torus shell. If the torus shell is made of fabric, however, its resistance to compression is nil. The pressure times the cross-sectional area of the torus, therefore, must be greater than the hoop compression.

The possibility exists, however, that collapse of the torus ring still may occur. There are two criteria that an inflated member subjected to external compressive loads must satisfy.[1] In the case of axially loaded straight columns, they are

$$P \leq pA \tag{1}$$

$$P \leq P_E \tag{2}$$

where P_E is the Euler buckling criterion (intermediate column buckling also may be possible, but there is insufficient data to establish a range). When shear flexibility can be neglected

$$P_E = \pi^2 EI/L^2 \tag{3}$$

where L is the effective length of the column. Except insofar as EI may be influenced by the pressure, Eq. 2 is therefore independent of p. It follows that, if P_E is less than pA, the column can buckle and collapse even though superficially every part of it is in tension. Inasmuch as the equations for buckling of rings are derived in a similar manner to those for straight members, and since (as shown later) their form is the same as that of the classical Euler buckling formula for straight members, the identical phenomenon can be expected in inflated toroidal membrane shells subjected to radial compression. Since fabric usually has a rather low modulus of elasticity (E), this mode of failure turns out to be critical in a good many fabric structures. Since the shearing stiffness of fabrics can be quite low, however, it is necessary to consider also the influence of shear flexibility on the buckling load.[1] Shear stiffness data is obtained from tests of straight members, and

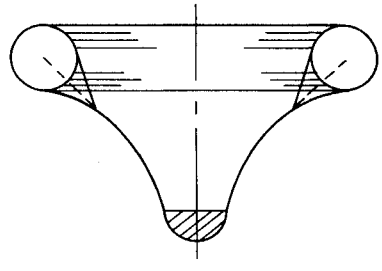

Fig. 1 Toroidal drag body.

Presented as Paper 70-1198 at the AIAA Aerodynamic Deceleration Systems Conference, Dayton, Ohio, September 14–16, 1970; submitted Sept. 25, 1970; revision received July 22, 1971; the author is indebted to his colleague, D. C. Goubeaux, for supervising the tests and coauthoring the report on which much of this paper is based.

Index categories: Aircraft Deceleration Systems; Structural Stability Analysis.

* Section Head, Structural Analysis. Member AIAA.
† TM, Goodyear Aerospace Corp., Akron, Ohio.

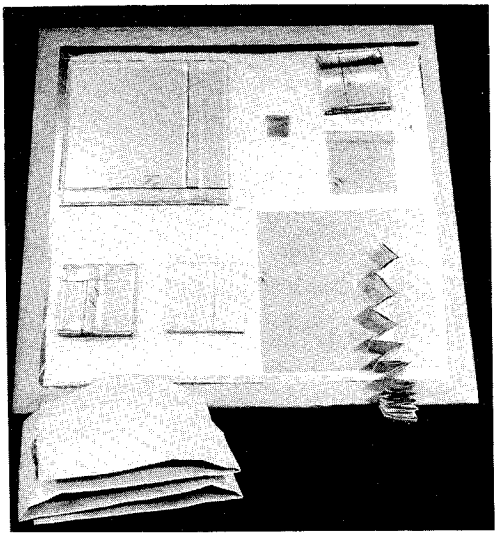

Fig. 2 Specimens during and after packaging.

the results of both analysis and experiment on inflated columns are pertinent to the problem at hand.

In the analysis of fabric structures, it is customary to treat the thickness (which, because of both the inhomogeneity of fabric and its generally negligible bending stiffness usually has no great significance) as unity; this practice is followed here. Then stresses and moduli are conveniently defined in units of pounds per inch and moments of inertia in cubic inches.

Effect of Shear Flexibility

Single-ply fabric, such as that used in most aerodynamic decelerators, has a very low shear modulus that is approximately equal to[2]

$$G = G_o + f_t \tag{4}$$

where G_o represents the inherent shear stiffness of the material. It has been shown[1] that, if G' is referred to as the enclosed cross-sectional area

$$G'A = \lambda = pA + kG_o \tag{5}$$

which is a convenient form for beam and column analysis. For a circular cross-section of constant thickness[1]

$$k = \pi r \tag{6}$$

The form of Eq. 5 results from considering that the tension component of G is able to resist displacement in any direction, while the resistance (G_o) in a thin shell is assumed effective only in the direction of the tangent to the shell. The result $G' = p$ when $G_o = 0$ has been shown by several approaches.[2-4] In Ref. 1, the following equation for buckling of an inflated column shear flexibility is obtained:

$$P_c = \tfrac{1}{2}[\lambda + 2P_E - (\lambda^2 + 4P_E{}^2)^{1/2}] \tag{7}$$

Equation 7 was developed from the first of two analyses of the effect of shear flexibility by Timoshenko and Gere.[5] The second analysis is, however, a little more accurate and, surprisingly, for inflated members leads to a simpler form of Eq. 7.

According to this second analysis (which takes into account the shear deflection term in defining the shear component),

$$P_c = [(1 + 4nP_E/AG')^{1/2} - 1]/(2n/AG') \tag{8}$$

in which n is a numerical factor such that AG'/n can be replaced by $pA - P + kG$ for pressurized thin-walled members.[1] Then, using Eq. 5, Eq. 8 becomes

$$P_c = \{[1 + 4P_E/(\lambda - P_c)]^{1/2} - 1\}/[2/(\lambda - P_c)] \tag{9}$$

Combining terms and squaring gives

$$(\lambda + P_c)^2 = (\lambda - P_c)(\lambda - P_c + 4P_E) \tag{10}$$

Expanding and reducing gives

$$P_c\lambda = P_E(\lambda - P_c) \tag{11}$$

and finally

$$P_c = P_E\lambda/(\lambda + P_E) \tag{12}$$

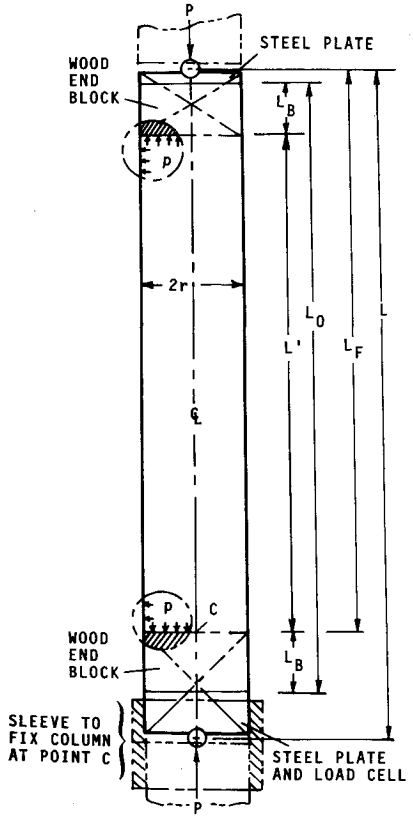

Fig. 3 Column-test geometry.

Confirmation of Theory by Test

To check the applicability of the foregoing theory, a series of tests was carried out at Goodyear Aerospace in 1965. Three materials of widely differing characteristics were selected: 1) Dacron-cloth, neoprene coating, single ply, weight: 7 oz/sq yd, specification strength: 170 lb/in. warp, 150 lb/in. fill, base cloth: 4 oz/sq yd, plain weave: 220 × 220 denier, 60 × 55 count, fill longitudinal all specimens; 2) Type 304 stainless steel cloth, silicone coating, single ply: 0.0016-in.-diam. monofilament wire, 200 × 200 count: warp longitudinal all specimens. 3) Mylar film, $\frac{1}{2}$-mil (0.0005 in.) thick, roll direction longitudinal all specimens.

To determine the material properties needed in the theory, some supplementary tests had to be made. Two cylinders of each material were made for torsion tests (to determine the

Table 1 Packaged volume/theoretical volume ratios

Specimen	Mylar	Dacron-neoprene	Metal fabric
Column	1.165	1.083	1.273
Torsion	1.203	1.197	1.229
Bending[a]	1.218	1.186	1.122

[a] Test results from the bending specimens are reported in Ref. 10.

Table 2 Summary of shear stiffness data from torsion tests

Material	lb/in.	p, psi	$pR/2$, lb/in.	G_o, lb/in.
Dacron				
Unpackaged	126	3.33	10	116
Packaged	128	3.33	10	118
Mylar				
Unpackaged	156	0.3056	1	155
Packaged	156	0.3056	1	155
Metal fabric				
Unpackaged	11.4	1.165	3.5	7.9
Packaged	26.5	0.778	2.3	24.2

shear modulus) and two each for the column tests. All specimens were made with two diametrically opposite longitudinal seams to minimize eccentricity. The torsion cylinders each were 12 in. in diameter and 36 in. long, with a 20-in. gage length. The column specimen dimensions were designed 1) to yield column buckling in a range to best check the theory—that is, to give a slenderness ratio high enough to get Euler buckling but low enough that shear flexibility as affected by inflation pressure would be significant (estimated material properties were used for this purpose) and 2) to stay within the limits of the available testing equipment.

The column tests were carried out in an Instron testing machine, not only to measure the loads with exactness but also to measure axial deflections, since these were needed to obtain values for the specified conditions. It was possible to make repeated tests of the same specimen since the deflection after buckling was limited by the travel of the machine head.

Packaging

To investigate the effect of packaging, one of each kind of specimen was subjected to a simulated packaging. Each cylinder was pressed flat, avoiding creasing at the seams, folded once with a lengthwise crease, and then folded accordion style into a square package (Fig. 2). The folded packages then were subjected to a pressure of 11.53 psi by a vacuum bag method for 5 days before being tested. The packaged volume was obtained by making a mold around the packaged specimen and later measuring the amount of mercury it would hold. Table 1 gives the packaging ratios obtained. An attempt to correlate this data with such parameters as fabric thickness and specimen diameter was made, but this attempt was unsuccessful.

Basic Test Data

The values of G_o obtained from the torsion tests are summarized in Table 2. G_o has been corrected for the stiffening effect of the pressure. Figure 3 shows the important column dimensions and test setup. The lower end was designed so that it either could be clamped or free to pivot on the spherical balls. The upper end remained free to rotate. Wooden end blocks were cemented inside the ends of the columns to facilitate attachment to the end plates in which the $\frac{3}{4}$-in.-diam balls were socketed. In the fixed-end mode, this was taken into account by considering the end fixed at the top of the end block. In the pinned end mode, the effect of this hardware was neglected. Figure 4 shows the unpackaged Mylar specimen in the testing machine under maximum load; Fig. 5 shows the other five column specimens. Figures (6–8) show representative load-deflection curves for each of the three materials.

Effect of Nonlinearity

All curves in Figs. 6–8 exhibit considerable nonlinearity so that a question arises as to what should be used as E for the column in Eq. 3. According to the Engesser-Karman theory (Ref. 5, pp. 175–178) a reduced modulus that is a function of

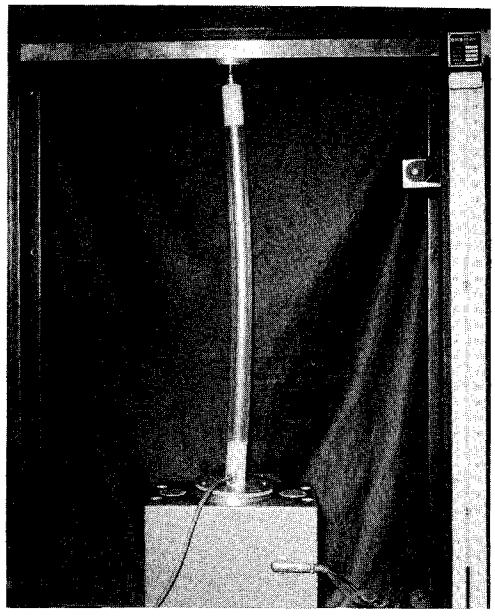

Fig. 4 Unpackaged Mylar column under maximum load in instron machine.

the initial modulus, the tangent modulus, and the column cross section should be used. The tangent modulus theory (Ref. 5, pp. 178–179) is generally better for tests under a steadily increasing load (as has been shown by Shanley[6]) and gives a lower bound while the reduced modulus theory gives an upper bound. For a circular thin-walled section, the reduced modulus cannot be expressed explicitly, and only the tangent modulus theory will be used.

To obtain a tangent modulus, a column shorter than the column of interest must be tested, since the load deflection curve for any column has a horizontal tangent—which would indicate a zero modulus—at its buckling load. It was to overcome this difficulty that the fixed-end capability was provided. The effective length for the fixed-pinned mode was taken as 0.7 L_F (Fig. 3).

Effect of Crookedness

Three of the columns were found not perfectly straight, and corrections were made in the calculation of theoretical buckling loads. The unpackaged Mylar column had a slight bow and Eq. 38 of Ref. 1 was used

$$(pA - P_{ce})I/sc = P_{ce}e \sec[(\pi/2)(P_{ce}/P_c)^{1/2}] \qquad (13)$$

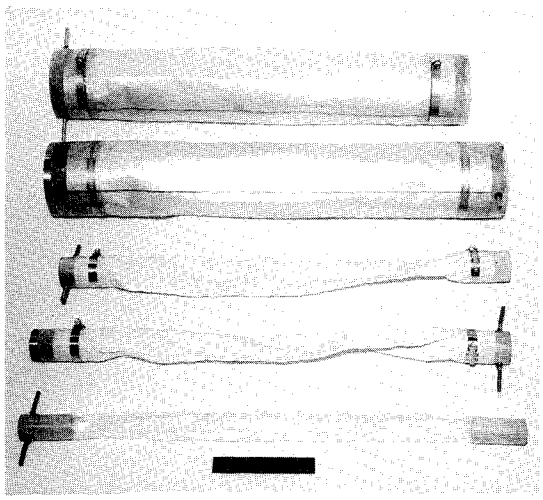

Fig. 5 Assembled column test specimens.

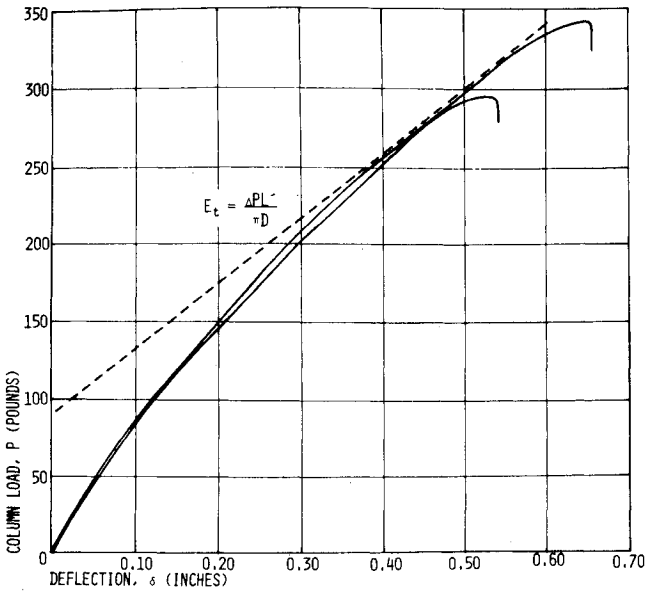

Fig. 6 Load-deflection curves (unpackaged Dacron columns).

This was solved by trial for P_{ce} with the eccentricity $e = 0.024$ in.

Slight kinks were found in the two metal fabric columns as a resu t of an end block being installed a little crookedly. This problem is treated by Timoshenko and Gere (Ref. 5, p. 34) by obtaining an equivalent side load

$$Q = P_e L/a(L - a) \tag{14}$$

which can then be used in Eq. 15 (Ref. 5, p. 5)

$$y = \frac{Q \sin ja}{Pj \sin jL} \sin jx - \frac{Qax}{PL} \quad [\text{for } x < (L - a)] \tag{15}$$

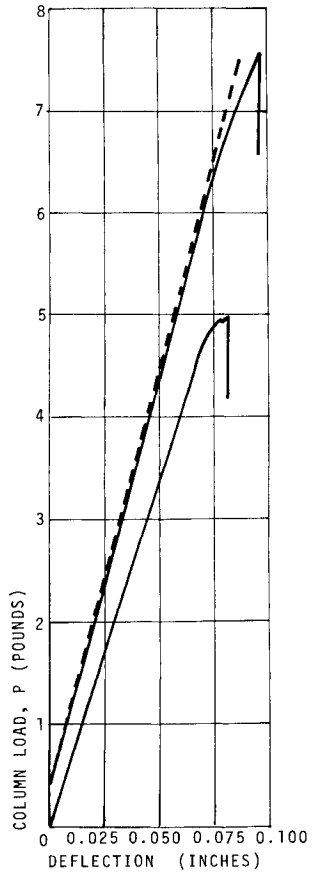

Fig. 7 Load-deflection curves (packaged Mylar columns).

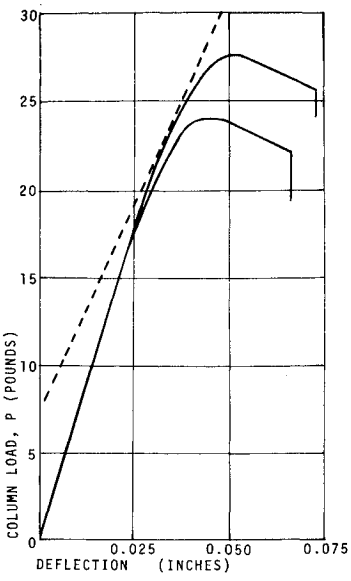

Fig. 8 Load-deflection curves (packaged metal columns).

in which

$$j^2 = P/EI = (P/P_c)\,\pi^2/L^2 \tag{16}$$

By substituting Eq. 14 into Eq. 15 and noting that $M = Py$, and equating M to the allowable moment given by Eq. 36 of Ref. 1, one finds

$$(pA - P_c)\frac{1}{sc} = \frac{P_c eL}{a(L - a)}\left(\frac{\sin ja \sin jx}{j \sin jL} - \frac{ax}{L}\right) \tag{17}$$

The location of the maximum moment is not obvious. An exact determination of x is not essential to the determination of P_c with sufficient accuracy for practical purposes. With $a > L/2$, x must be between $L/2$ and a. For both the metal fabric columns, x was assumed to be $0.6L$.

Comparison of Theory and Experimental Data

The calculated buckling loads are compared with the test results in Table 3. The test values range from 22% above the theoretical for the unpackaged Dacron-neoprene column to 5.5% below for the packaged metal fabric column (the only one to fail below the predicted value). If it is assumed that I for the unpackaged Dacron-neoprene should be increased (while E_t is at the same time decreased) since it buckled across a seam, the maximum deviation will be reduced to 15%. In any case, the deviations are within the scatter ordinarily found in column testing. Packaging had little effect on the results. In Fig. 9, these results are shown graphically. The agreement between theory and test appears good, but in the case of the metal fabric column pA is undesirably close to P_c for purposes of such comparison. This makes it necessary to observe that the local crippling strength of the metal fabric is not negligible if shear flexibility is neglected. Using as an approximation the familiar equation

$$f_{cr} = 0.3E/r \tag{18}$$

(in which $E = Et$ in the more usual notation) one finds

$$P_{cr} = 0.6\pi Et + pA \tag{19}$$

Taking the value of t as two wire diameters (0.0032 in.) gives $P_{cr} = 0.6\pi(1759)(0.0032) + 34.2 \approx 45$ lb, or about $0.82P_E$. This consideration is not significant for the other two materials.

Application of Theory

Accepting the correctness of the theory, some obstacles may remain to prevent its ready application. The value of the

Table 3 Column data and buckling loads

Name	Units	Comment	Mylar (t = 0.0005 in.)		Metal fabric		Dacron-neoprene	
			Unpackaged	Packaged	Unpackaged	Packaged	Unpackaged	Packaged
L	in.	Pin ends	32.58	32.58	32.52	32.58	32.52	32.55
$2r$	in.		1.523	1.512	2.032	2.039	5.15	5.15
I	in.		1.390	1.358	3.29	3.33	53.6	53.6
A	in.		1.822	1.796	3.243	3.270	20.82	20.82
p	psi		4.89	4.89	10.5	10.5	17.0	17.0
E	lb/in.	Est	350	350	2500	2500	785	785
		Meas	424	405	1759	1759	635	635
G_o	lb/in.	Est	134.5	134.5	30	30	34	34
		Meas	155	155	8	24	116	118
e	in.	Eccentricity	0.024	0	0.099	0.087	0	0
pA	lb		8.90	8.78	34.0	34.3	354	354
			379	376	59.3	111.7	1293	1308
P_E*	lb	Est	4.52	4.41	76.8	77.5	242	242
		Meas	5.48	5.10	54.0	54.5	317	318
P_c*	lb	Est	4.41	4.41	48.4	48.4	242	242
		Meas	5.40	5.03	28.2	36.6	255	256
P_c	lb	Test	5.45	5.47	32.5†	34.7†	310	295

tangent modulus E_t, in compression of an inflated member, is not generally available, and an estimate may have to be made from tensile data. In the present instance, the Dacron-neoprene fabric was the same as had been tested biaxially to determine its properties in Ref. 7, and the metal fabric, though not identical to those tested in Ref. 7, was sufficiently similar that estimates could be made by ratioing wire cross-sectional areas. The actual values of the tangent modulus might be expected to be lower, and they were. For the Mylar, less nonlinearity would be expected, but it was not anticipated that the tangent modulus would be higher than the value of E estimated from Ref. 8, as Table 3 shows. The value of G_o for the Mylar also was estimated lower from Ref. 8 than from the present tests, which may suggest that the Mylar was somewhat thicker than the nominal 0.0005 in. assumed.

Extension of Theory to Ring Buckling

A ring subjected to radial compression may buckle either in its own plane or out of that plane. Timoshenko and Gere (Ref. 5, pp. 289–292, 317–318) discuss both problems without considering shear flexibility. For in-plane buckling, if one assumes that the external radial load remains normal to the distorted centerline of the ring after distortion

$$N_c = 3EI_1/R^3 \tag{20}$$

If instead one assumes that the external load remains acting at the centerline of the original ring, Nicolai[9] has shown that

$$N_c = 9EI_1/2R^3 \tag{21}$$

For buckling out-of-plane, three alternate solutions are known. If the external load remains acting in the original plane of the ring after distortion[9]:

$$N_c = 3EI_2/R^3 \tag{22}$$

If the external load acts along the centerline of the distorted ring but parallel to the original plane (Ref. 5, pp. 289–292 and pp. 317–318 and Ref. 9),

$$N_c = 9EI_2/R^3(4 + EI_2/GJ) \tag{23}$$

If the external load remains directed toward the center of the original ring though acting at the centerline of the deflected ring (Ref. 5, pp. 289–292 and 317–318 and Ref. 9)

$$N_c = 12EI_2/R^3(4 + EI_2/GJ) \tag{24}$$

In the derivation of all of Eqs. (20–24), R is assumed much greater than r. The form of Eqs. (20–22) is the same as Eq. (3). They differ from Eq. (3) only by a numerical constant, since the critical load, $P_c = N_cR$, acts on every cross section and since R is a measure of the length of the member. It is thus logical to assume that P_c for a ring is reduced by shear flexibility in the same way that the buckling load of a straight column is reduced. Then, rewriting Eq. (12) to apply to annular inflated members

$$N_cR = (N_cR)_E\lambda/[\lambda + (N_cR)_E] \tag{25}$$

Equations (23) and (24) are also similar in form to Eq. (3), but include the bending/torsion stiffness ratio EI/GJ. The application of Eq. (25) to loadings of these types still seems plausible but perhaps more doubtful than for the previous three cases. A rigorous theoretical proof of Eq. (25) is beyond the intended scope of this paper.

Application to Simple Torus

Returning now to the toroidal drag body of Fig. 1, in which the ring is compressed by the radial component of the skirt tension, if the torus is of circular cross-section with radius r, the circumferential (as distinguished from meridional) stresses in the torus due to internal pressure are uniform

$$f_t = pr/2 \tag{26}$$

Since $I_1 = I_2$ for a circle, Eq. 23 is assumed to give the critical

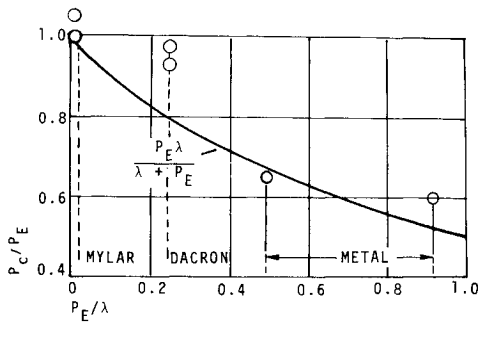

Fig. 9 Comparison of theory and test results for inflated columns.

buckling load (provided the resultant compressive forces act at the ring centerline) with

$$I_2 = \pi r^3 \tag{27}$$

$$J = 2\pi r^3 \tag{28}$$

Then, from Eqs. (23), (5), (25), and (26),

$$N_c R + \frac{9\pi E r^3 (pr + G_o)(pr + 2G_o)}{R^2(pr + G_o)(4pr + 8G_o + E) + 9Er^2(pr + 2G_o)} \tag{29}$$

If the skirt tension resultant does not pass through the center of the ring cross section (as in Fig. 1), uniformly distributed couples exist around the ring, which result in a bending moment that affects the critical buckling load. A combined bending-compression buckling is, however, beyond the scope of this paper. The equations for buckling of cones or noncircular toroids are different, but the approach is similar.

References

[1] Topping, A. D., "Shear Deflections and Buckling Characteristics of Inflated Members," *Journal of Aircraft*, Vol. 1, No. 5, Sept.–Oct. 1964, pp. 289–292.

[2] Topping, A. D., "An Introduction to Biaxial Stress Problems in Fabric Structures," *Aerospace Engineering*, Vol. 20, No. 4, April 1961; pp. 18–19, 53–57.

[3] Leonard, R. W., Brooks, G. W., and McComb, H. G., "Structural Considerations of Inflatable Re-entry Vehicles," TN D-457, Sept. 1960, NASA.

[4] Leonard, R. W., McComb, H. G., Zender, G. W., and Stroud, W. J., "Analysis of Inflated Re-entry and Space Structures," *Symposium on Recovery of Space Vehicles*, Los Angeles Section of The Institute of Aeronautical Sciences, Los Angeles, Calif., Aug. 31–Sept. 1, 1960.

[5] Timoshenko, S. and Gere, J. M., "Theory of Elastic Stability," 2nd ed., McGraw-Hill, New York, 1961, pp. 132–135.

[6] Shanley, F. R., "Weight-Strength Analysis of Aircraft Structures," 2nd ed., Dover, New York, 1960, pp. 323–342.

[7] Foerster, A. F. et al., "Analytical and Experimental Investigation of Coated Metal Fabric Expandable Structures for Aerospace Applications," ASD-TDR-63-542, Aug. 1963.

[8] Seide, P., Weingarten, V. I., and Morgan, E. J., "Final Report on the Development of Design Criteria for Elastic Stability of Thin Shell Structures," AFBMF/TR-61-7, Dec. 31, 1960.

[9] Nicolai, E. L., "Stability Problems in Theory of Elasticity," *Zeitschrift fur Angewandte Mathematik and Mechanik*, Vol. 3, 1923, pp. 227–229.

[10] Topping, A. D., "Buckling Resistance of Inflated Cylinders in Bending," *Transactions of the Third Aerospace Expandable and Modular Structures Conference*, AF APL TR 68-17, 1967, pp. 147–165.

NOVEMBER 1971 J. AIRCRAFT VOL. 8, NO. 11

Airfoils in Two-Dimensional Nonuniformly Sheared Slipstreams

G. R. Ludwig* and J. C. Erickson Jr.†
Cornell Aeronautical Laboratory Inc., Buffalo, N. Y.

A theoretical and experimental program has been conducted to investigate the aerodynamics of an airfoil in a two-dimensional nonuniformly sheared slipstream. A mathematical model has been developed to predict airfoil pressure distributions in such a slipstream and has been used successfully for slipstreams with moderate shear. Pressure distributions over a wide angle-of-attack range have been measured experimentally on an airfoil at each of seven different locations in a highly sheared two-dimensional slipstream. Study of the pressure distributions obtained on the airfoil at a location slightly above the flow centerline and also at a location slightly below the flow centerline indicates that the large effects on stalling characteristics are due to differences in the upper surface pressure distributions. These pressure distributions are affected by the freestream shear. Moreover, in the data obtained for airfoils located near the flow centerline, the differences in the lift appear to be caused primarily by differences in the stagnation pressure of the streamline which intersects the airfoil. This stagnation pressure is a function not only of airfoil location relative to the slipstream, but also of the angle of attack of the airfoil.

Nomenclature

c = airfoil chord, Fig. 1a
C_l = sectional lift coefficient
C_p = pressure coefficient
h = vertical height of airfoil midchord above tunnel centerline, Fig. 1
L = vertical distance from tunnel centerline to tunnel floor or ceiling, Fig. 1a
r = vertical distance from tunnel centerline to point of maximum velocity in undisturbed nonuniformly sheared slipstream profile, Fig. 1b
x = coordinate along axis parallel to tunnel floor and ceiling, positive downstream; $x = 0$ at airfoil leading edge
y = coordinate perpendicular to x axis, positive upward; $y = 0$ at tunnel centerline
α = airfoil angle of attack, positive leading edge up, Fig. 1
ψ = stream function, Eq. (1)
$(\ )_R$ = coefficient referred to freestream velocity at airfoil midchord position
$(\ )_S$ = coefficient referred to freestream velocity along airfoil stagnation streamline

Presented as Paper 71-94 at the AIAA 9th Aerospace Sciences Meeting, New York, January 25–27, 1971; submitted February 8, 1971; revision received July 23, 1971. This research was supported by the U.S. Army Research Office-Durham on Contract DAHC04-67-C-0071. The authors wish to acknowledge the contributions of W. G. Brady to the theoretical investigation and of J. Nemeth Jr., to the performance of the experiments.

Index categories: Rotary Wing and VTOL Aerodynamics; Jets, Wakes and Viscid-Inviscid Flow Interactions.

* Principal Aeronautical Engineer. Member AIAA.
† Research Aeronautical Engineer. Member AIAA.